Ion-induced folding of the hammerhead ribozyme: a fluorescence resonance energy transfer study

Gurminder S.Bassi, Alastair I.H.Murchie, Frank Walter, Robert M.Clegg[1] and David M.J.Lilley[2]

CRC Nucleic Acid Structure Research Group, Department of Biochemistry, The University, Dundee DD1 4HN, UK and [1]Abteilung Molekulare Biologie, Max-Planck-Institut für Biophysikalische Chemie, Am Fassberg 11, D-37077 Göttingen, Germany

[2]Corresponding author
e-mail: dmjlilley@bad.dundee.ac.uk

The ion-induced folding transitions of the hammerhead ribozyme have been analysed by fluorescence resonance energy transfer. The hammerhead ribozyme may be regarded as a special example of a three-way RNA junction, the global structure of which has been studied by comparing the distances (as energy transfer efficiencies) between the ends of pairs of labelled arms for the three possible end-to-end vectors as a function of magnesium ion concentration. The data support two sequential ion-dependent transitions, which can be interpreted in the light of the crystal structures of the hammerhead ribozyme. The first transition corresponds to the formation of a coaxial stacking between helices II and III; the data can be fully explained by a model in which the transition is induced by a single magnesium ion which binds with an apparent association constant of 8000–10 000 M^{-1}. The second structural transition corresponds to the formation of the catalytic domain of the ribozyme, induced by a single magnesium ion with an apparent association constant of ~1100 M^{-1}. The hammerhead ribozyme provides a well-defined example of ion-dependent folding in RNA.

Keywords: fluorescence/metal ions/ribozyme/RNA folding

Introduction

RNA-induced catalysis provides a fascinating challenge in chemical biology—to explain the generation of catalytic activity in terms of the structure of the folded RNA (Eckstein and Lilley, 1996). Because of their relative simplicity, the small nucleolytic RNA species are especially suitable for detailed study. Examples of such ribozymes are found in plant viroids (Forster and Symons, 1987; Hazeloff and Gerlach, 1988), the transcript of newt satellite DNA (Epstein and Gall, 1987), tobacco ringspot virus satellite RNA (Feldstein *et al.*, 1989; Hampel and Tritz, 1989) and the hepatitis delta virus (Sharmeen *et al.*, 1988). The best studied small nucleolytic RNA is the hammerhead ribozyme (reviewed in Thomson *et al.*, 1996). These molecules undergo a site-specific cleavage,

requiring only magnesium or similar cations for activity (Dahm and Uhlenbeck, 1991), and can be reduced to one or more pieces of RNA comprising ~50 nucleotides.

Phosphodiester cleavage occurs by a transesterification reaction, whereby the oxygen atom of the 2′-hydroxyl attacks the 3′-phosphorus by an S_N2 mechanism. The products are 5′-hydroxyl and 2′,3′-cyclic phosphate termini (Hutchins *et al.*, 1986; Uhlenbeck, 1987), and the reaction proceeds with inversion of configuration at the phosphorus (van Tol *et al.*, 1990; Koizumi and Ohtsuka, 1991; Slim and Gait, 1991). Cleavage in the presence of magnesium ions is inhibited by R_p thiophosphate substitution (Slim and Gait, 1991), but is restored if the ion is replaced by manganese (Dahm and Uhlenbeck, 1991). This indicates that the metal ion, possibly as a hydroxide (Dahm *et al.*, 1993), is bound to the *pro-R* oxygen atom of the phosphate, where it could increase the nucleophilicity of the 2′-hydroxyl and stabilize the transition state of the reaction.

Inspection of a model shows that the structure of A-form RNA does not provide the alignment required for the transition state of an S_N2 mechanism. A major source of rate enhancement could be distortion or strain of the local RNA structure to facilitate the achievement of the conformation required for in-line attack, and the ribozyme might therefore be expected to fold into a conformation that achieves this pre-activation of the phosphodiester bond. It is probable that metal ions will have two roles in the generation of catalytic activity. Nucleic acids are highly charged polyelectrolytes, and folding generally requires the participation of metal ions. These can interact in an atmospheric manner to provide overall charge neutralization, but in the course of folding, cavities with highly negative electrostatic potentials may be formed that can bind multivalent ions in a more localized site-specific manner (Klement *et al.*, 1991). Thus it is probable that metal ions will induce the folding into the geometry required to facilitate the trajectory into the transition state, and will also bind at a specific location(s) where they can participate directly in the chemistry of the cleavage reaction. A given metal ion may fulfil either a structural or catalytic role, or in principle, both.

The hammerhead ribozyme can be regarded as a kind of three-way RNA junction, where three helical sections are connected by the conserved core comprising formally single-stranded sections of 7, 3 and 1 nucleotide [a $HS_1HS_7HS_3$ junction (Lilley *et al.*, 1995)] (Figure 1A). The sequence has been subjected to extensive *in vitro* mutation to reveal the positions critical for self-cleavage (Ruffner *et al.*, 1990), and in general these are located in and around the single-stranded segments. The position of self-cleavage is located within the shortest single-stranded section. The core region has been extensively studied by selective base and ribose substitution to remove or alter
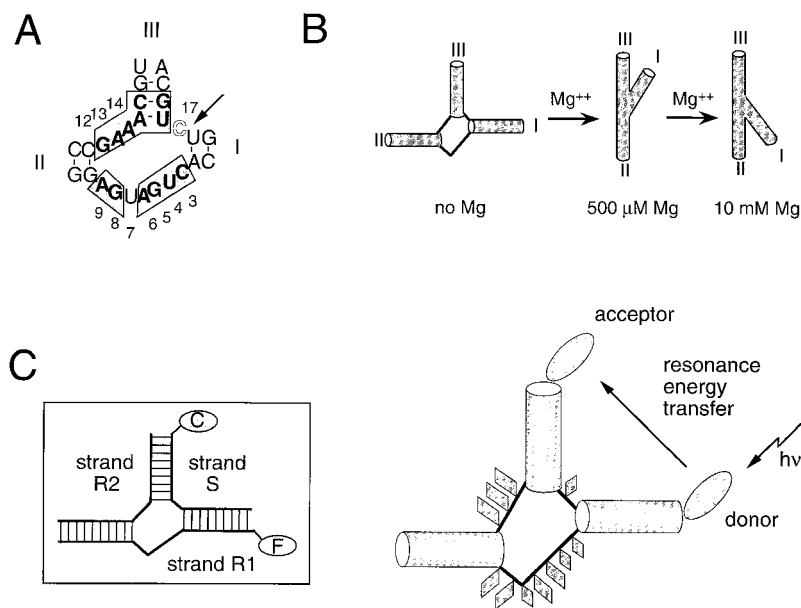
Fig. 1. The hammerhead ribozyme and its ion-dependent folding. (**A**) The sequence of the core of the hammerhead ribozyme, showing the conserved sequences (boxed). The arrow indicates the position of self-cleavage. In the spectroscopic experiments, C_{17} (open type) was replaced by deoxyribocytosine to prevent self-cleavage occurring in the presence of magnesium ions. The bases of the core are numbered according to Hertel *et al.* (1992), and the helices are conventionally numbered I, II and III. (**B**) The two-stage reaction path of ion-dependent folding of the hammerhead ribozyme deduced from comparative gel electrophoresis experiments (Bassi *et al.*, 1995). These experiments indicated that low concentrations of magnesium ions induce a folding of the hammerhead such that a large angle is subtended between helices II and III, with the smallest angle between helices I and III. Upon further increase in magnesium ion concentration over the 1–20 mM range, there is a further change in the global structure such that helix I rotates around to subtend the smallest angle with helix II. (**C**) The study of hammerhead folding by fluorescence resonance energy transfer. Fluorescein and Cy-3 are covalently attached via flexible six-carbon linkers to the 5′-termini of different component strands of the hammerhead structure. This places the fluorophores at the distal ends of different helical arms. In the example illustrated, the fluorescein (F) and Cy-3 (C) fluorophores attached to the 5′ ends of the strands R1 and S respectively, locating the fluorophores at the ends of helices I and II. From this the efficiency of energy transfer can be measured spectroscopically; the efficiency is inversely related to the scalar length of the end-to-end vector I–II. This is repeated for the vectors I–III and II–III.

specific functional groups (Olsen *et al.*, 1991; Fu and McLaughlin, 1992a,b; Paolella *et al.*, 1992; Williams *et al.*, 1992; Yang *et al.*, 1992; Fu *et al.*, 1993; Grasby *et al.*, 1993; Seela *et al.*, 1993; Tuschl *et al.*, 1993). Those affecting the catalytic efficiency of the ribozyme are located in the single-stranded sections.

The structure of the hammerhead is highly dependent on the type and concentration of metal ions present. Using comparative gel electrophoresis we have shown (Bassi *et al.*, 1995) that the global structure undergoes a two-stage folding transition upon addition of magnesium ions (Figure 1B). In the absence of added ions, the structure is essentially that of the conventional depiction of the hammerhead. Upon addition of 500 μM magnesium ions, the hammerhead folds into a structure in which there is a large angle (presumed coaxial stacking) between helices II and III, and over the range 1–15 mM magnesium ions there is a further folding in which helix I seems to rotate around from being directed in a similar direction to helix III to being close to helix II. The position of self-cleavage must lie close to the axis of this rotation.

The final form adopted in ≥10 mM magnesium ions is in good agreement with the global form of the structure seen in the two crystal structures of the hammerhead (Pley *et al.*, 1994; Scott *et al.*, 1995), and with structures deduced from fluorescence resonance energy transfer (Tuschl *et al.*, 1994) and transient electric birefringence (Amiri and Hagerman, 1994). The short distance between helices I and II is consistent with crosslinking studies (Sigurdsson

et al., 1995). In the crystal structures (Pley *et al.*, 1994; Scott *et al.*, 1995), helices II and III are associated coaxially through the formation of a paired region between the $G_{12}A_{13}A_{14}$ sequence between helices II and III, and the $U_7G_8A_9$ sequence found at the 3′ end of the long single-stranded section of the core. It seems very probable that the formation of this structure would correspond to the low-magnesium transition. The second magnesium-induced transition occurring over the 1–15 mM region is likely to correspond to the formation of domain I in the crystal structures, formed by the $C_3U_4G_5A_6$ sequence occurring at the 5′ end of the long single-stranded section of the core.

Our previous conclusions were based on deductions from relative electrophoretic mobilities. While this has proved to be a powerful and reliable technique in the analysis of branched nucleic acids (Duckett *et al.*, 1988, 1995; Welch *et al.*, 1995), it has an incomplete theoretical basis at present, and we sought an alternative approach to test the folding model. In this study we have applied a spectroscopic technique to provide complementary information. We find that this confirms and extends our earlier conclusions.

Results and discussion

Study of ion-induced folding of RNA by fluorescence resonance energy transfer

We have used fluorescence resonance energy transfer (FRET) to follow the folding transitions induced by the

addition of magnesium ions. For this, we have constructed a series of hammerhead-related species comprising the core (with deoxyribose substitution at C_{17} to prevent self-cleavage) and three arms each of 10 bp in length. Donor and acceptor fluorophores have been attached to the 5′ ends of arms in a pairwise manner (Figure 1C), in order to follow the change in length of the vector connecting the termini of the chosen arms as a function of magnesium concentration; this length is proportional to the angle subtended between the same arms. Energy transfer results from a dipolar coupling between the transition moments of the two fluorophores, and the efficiency (E_{FRET}) is inversely dependent on the distance between them,

$$E_{FRET} = \frac{1}{[1+(R_0/R)^6]} \qquad (1)$$

where R is the distance between the two fluorophores, and R_0 is characteristic of the fluorophores used and is related to the distance at which E_{FRET} is half-maximal. For this study we have used fluorescein as the donor fluorophore and cyanine-3 (Cy-3) as the acceptor. Cy-3 is relatively constrained when attached to the RNA duplex; we have measured the anisotropy (r) as 0.270 in the presence of 90 mM Tris-borate pH 8.3, 25 mM NaCl. However, the fluorescein is relatively mobile ($r = 0.100$ in the presence of 90 mM Tris-borate pH 8.3, 25 mM NaCl) and thus dye orientation very probably does not complicate the straightforward interpretation of our FRET results. Each helix in the constructs terminates in a 5′CC sequence to provide a constant environment for the fluorophores; we have previously found that this provides a well-behaved environment for FRET measurements in nucleic acids (Murchie *et al.*, 1989; Clegg *et al.*, 1992, 1993). We have calculated efficiencies of FRET using the *(ratio)$_A$* method (Clegg, 1992), whereby the enhanced emission spectrum of the Cy-3 acceptor extracted from that of the double-labelled sample excited at 490 nm (primarily, but not exclusively, fluorescein excitation) is normalized to a second acceptor spectrum extracted from the spectrum of the same sample excited at 547 nm where only Cy-3 is excited. *(ratio)$_A$* is directly related to FRET efficiency, as explained in Materials and methods.

Neither the attached fluorophores nor the deoxyribose substitution of the terminal base pair (core distal) in each

helix affects the ability of the hammerhead constructs to function as active ribozyme species. We have constructed a hammerhead ribozyme from a radioactively 5′-^{32}P-labelled substrate strand (S′) with ribose substitution at C_{17} (therefore potentially competent in self-cleavage) hybridized to a large excess of 5′-fluorescein R1 strand
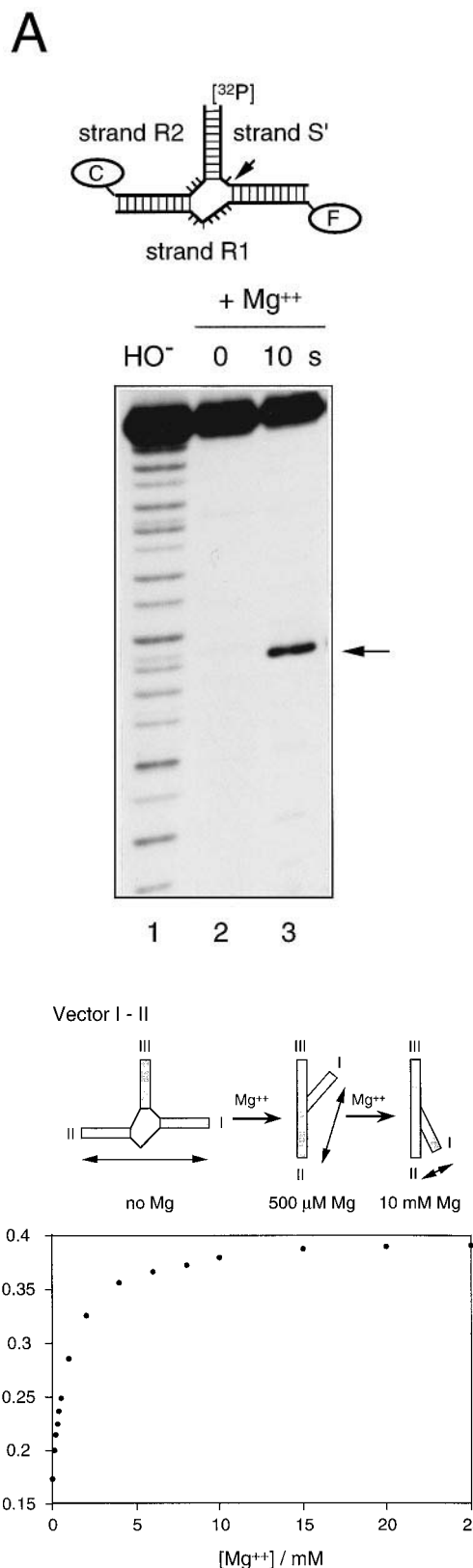
Fig. 2. FRET analysis for the end-to-end vector I–II of the hammerhead ribozyme as a function of magnesium ion concentration. (**A**) Ribozyme activity of the fluorophore-labelled hammerhead constructs. The self-cleavage activity was examined for a hammerhead construct identical to that used for the FRET analysis except for ribose substitution at C_{17}. Radioactively 5′-^{32}P-labelled ribose-substituted substrate strand S′ was incubated with a 100-fold excess of preincubated fluorescein-R1 and Cy-3-R2 strands in the presence of 25 mM MgCl$_2$ at 37°C. A sample was removed at zero time (track 2) and 10 s (track 3). A ladder was generated by hydroxide cleavage to act as a sequence marker (track 1). The position of self-cleavage is indicated by the arrow. Prolonged incubation with magnesium ions led to >85% cleavage. (**B**) Measured efficiency of energy transfer as a function of magnesium ion concentration. The scheme shows the expected behaviour of the end-to-end vector I–II on the basis of the original model for the ion-induced folding of the hammerhead ribozyme. The length is expected to shorten over the entire range of magnesium ion. The plot shows the variation in FRET efficiency as a function of magnesium ion concentration up to 25 mM. In accordance with the model, the FRET efficiency is found to increase (indicating a reducing end-to-end distance) over this complete range.
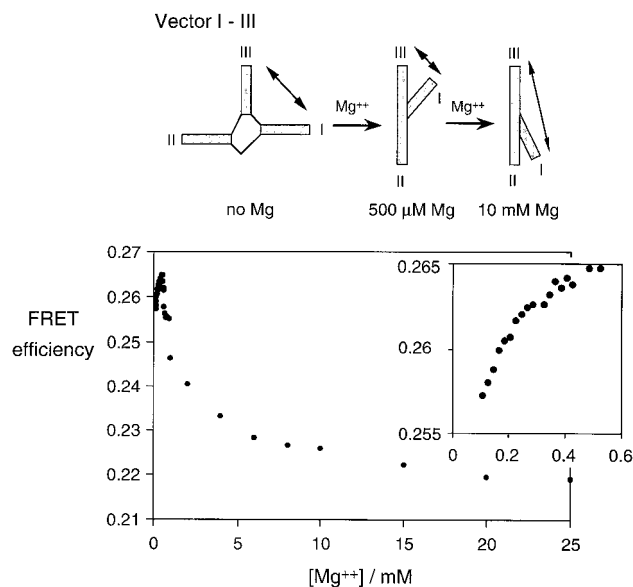
Fig. 3. FRET analysis for the end-to-end vector I–III of the hammerhead as a function of magnesium ion concentration. The hammerhead was constructed from fluorescein-labelled R1 strand and Cy-3-labelled S strand. The scheme shows the expected behaviour of the end-to-end vector I–III on the basis of the original model for the ion-induced folding of the hammerhead structure. The plot shows the variation in FRET efficiency as a function of magnesium ion concentration up to 25 mM. The insert shows an expansion of the plot for the region of magnesium ion concentration from 0–600 μM, over which there is a small but systematic increase in FRET efficiency.

Fig. 4. FRET analysis for the end-to-end vector II–III of the hammerhead ribozyme as a function of magnesium ion concentration. The hammerhead molecule was constructed from Cy-3-labelled R2 strand and fluorescein-labelled S strand. The scheme shows the expected behaviour of the end-to-end vector II–III on the basis of the original model for the ion-induced folding of the hammerhead. The plot shows the variation in FRET efficiency as a function of magnesium ion concentration up to 25 mM. Note that there is a sharp fall in efficiency within the first 1 mM range of magnesium ion concentration. This is seen more clearly in the insert, which shows an expansion of the plot for the region of magnesium ion concentration from 0–600 μM.

and 5′-Cy-3 R2 strand. Incubation under these single-turnover conditions in the presence of 25 mM magnesium ions at 37°C leads to cleavage at the correct site (Figure 2A).

Variation in end-to-end lengths during the ion-induced folding of the hammerhead

According to the model for the folding of the hammerhead, the length of vector I–II should shorten over the full range of magnesium concentration. Experimentally, we find that E_{FRET} increases over the whole range and reaches a plateau value by 15–20 mM magnesium (Figure 2B), in agreement with this model. The behaviour of the length of the I–III vector is predicted to be more complex. This distance should shorten in the first transition (up to 500 μM magnesium ions), but then lengthen in the second transition (1–15 mM). We find that there is a small initial increase in E_{FRET} up to 500 μM magnesium, followed by a reduction that once again reaches a plateau by 15–20 mM (Figure 3). This is consistent with a small shortening of the I–III distance in the first transition, followed by a significant lengthening in the second. The third vector is predicted to have a rather different character. Helices II and III are connected by the G.A scaffold, and are predicted to undergo coaxial alignment in the first transition, with a concomitant lengthening of the II–III vector length. This is essentially what is found. The value of E_{FRET} falls sharply with magnesium concentration, particularly in the range 0–500 μM, followed by a more modest reduction thereafter (Figure 4).

These results are fully consistent with the proposed two-stage mechanism for the ion-induced folding of the hammerhead ribozyme. The values for the efficiencies

under the three sets of conditions are summarized in Figure 5. In the absence of added magnesium ions, the lengths I–III and II–III are equal, but shorter than that for vector I–II. This is just what would be expected for the structure in which helices I and II are approximately colinear, with helix III projecting at right angles. This structure remains unaltered in the face of all mutations made in the core sequence (Bassi *et al.*, 1996), suggesting that the core is essentially unstructured at this stage. The global geometry of this species is consistent with the early transient electric birefringence study that found helices I and II to be colinear (Gast *et al.*, 1994); it is probable that the hammerhead assumed the unfolded structure under the conditions of that study.

Upon addition of magnesium ions, the vector II–III becomes the longest, consistent with the formation of coaxial stacking between helices II and III. The ultimate value of E_{FRET} for this vector is a little greater than that measured for an equivalent duplex, made by hybridizing the same R2 strand to its perfect complement ($E_{FRET} = 0.11$ in 10 mM magnesium ions). This suggests that while clearly coaxial, helices II and III are not exactly colinear in solution. The relative efficiencies for the I–II and I–III vectors fix the relative orientation of arm I in the structure. In the presence of 500 μM magnesium, the deduced relative lengths are I–II>I–III, while at 10 mM magnesium they have reversed so that the lengths I–III>I–II. This is consistent with a folding of the core that causes a rotation of arm I, and the final efficiency of the I–II vector indicates that this becomes the smallest angle observed under all conditions. Our conclusions do not depend on the determination of absolute distances, and in general each

no Mg   400 μM Mg   10 mM Mg
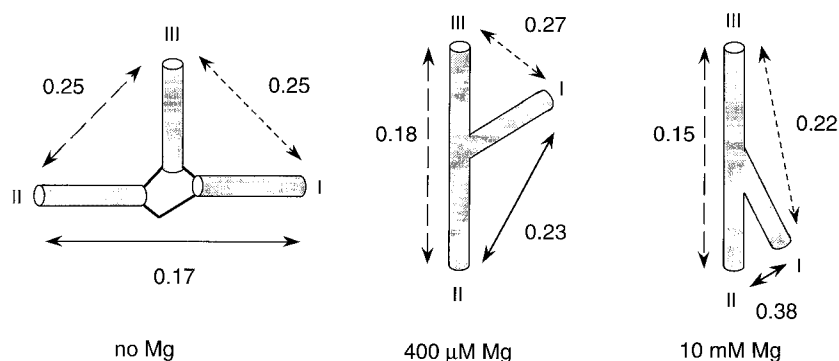
Fig. 5. Summary of the efficiencies of energy transfer for the three end-to-end vectors of the hammerhead in the presence of 0, 0.4 and 10 mM magnesium ions. The conditions reflect the three main stages of the ion-dependent folding process.

aspect of the model is supported by multiple observations, where efficiencies are both increasing and decreasing for different vectors.

Single-magnesium-induced conformational transitions

We have modelled each of the conformational transitions in terms of a single magnesium ion-induced folding, i.e.

$$RNA_{conformation1} + Mg^{2+} \leftrightarrow RNA_{conformation2} \cdot Mg^{2+} \quad (2)$$
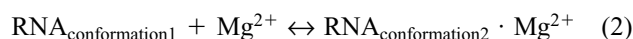
For this equilibrium, the proportion of the RNA in the magnesium-induced folded state (α) is given by:

$$\alpha = \frac{K \cdot [Mg^{2+}]}{(1 + K \cdot [Mg^{2+}])} \quad (3)$$

where K is the association constant

$$K = \frac{[RNA_{conformation2} \cdot Mg^{2+}]}{[RNA_{conformation1}] \cdot [Mg^{2+}]} \quad (4)$$

The FRET efficiencies for the shortening of vector II–III and the lengthening of vector I–III over the 0–500 μM range of magnesium concentrations were fitted to this model (Figure 6). Both sets of data are well fitted by this simple model, and yield association constants (10 000 and 7800 M^{-1} respectively) that are within the probable experimental error. The second transition was analysed in the same way, using the increase in E_{FRET} of the vector I–II over the 1–25 mM magnesium concentration range (Figure 7). Once again these data are well fitted by the simple model, giving an association constant (1100 M^{-1}) that is an order of magnitude lower than that for the low-magnesium transition. We conclude that the data are well explained by two successive single-magnesium ion-induced conformational transitions in the hammerhead RNA. More complex ion-binding schemes could be proposed that would be consistent with the fluorescence data, but the fitting demonstrates that single ion-binding models are sufficient to account for the observed data.

Location of metal ions important in the folding process

There is very good agreement between the original comparative gel electrophoresis experiments (Bassi *et al.*, 1995) and the present FRET data on the pathway of ion-induced folding of the hammerhead ribozyme, despite their very different physical bases. The folding occurs in
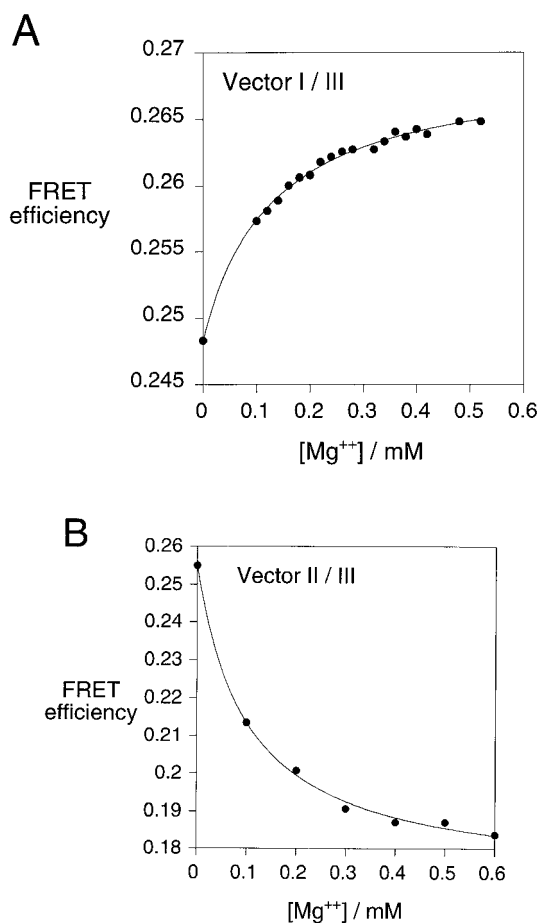
Fig. 6. Analysis of the low-magnesium ion transition of the hammerhead structure in terms of a single ion-binding model. The FRET efficiency data over the 0–600 μM magnesium ion range were fitted to the model described in the text, for end-to-end vectors II–III (**A**) and I–III (**B**). In each case the points are the experimental data, and the lines are the results of non-linear regression fitting to the single ion-binding model.

two distinct stages, each of which appears to be induced by the folding of a single magnesium ion. Sodium ions are ineffective in this role, as both the electrophoretic analysis (Bassi *et al.*, 1995) and the present FRET data indicate that the hammerhead remains in the unfolded conformation in the presence of 25 mM sodium ions. Clearly the present experiments cannot locate ions, but we can suggest some reasonable possibilities.
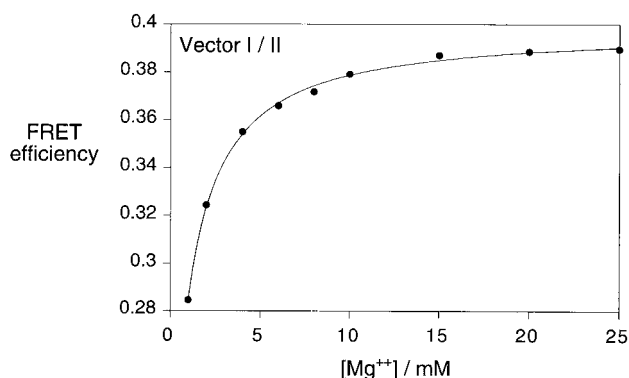
Fig. 7. Analysis of the high-magnesium ion transition of the hammerhead in terms of a single ion-binding model. The FRET efficiency data over the 1–25 mM magnesium ion range were fitted to the model described in the text, for end-to-end vector I–II. The points are the experimental data, and the line is the result of non-linear regression fitting to the single ion-binding model.

A good rationalization of our folding data is obtained if we identify the first (500 µM magnesium ions) transition with the formation of the GA stack [domain II according to McKay (Pley *et al.*, 1994)]. Mutations in the $G_{12}A_{13}A_{14}$ sequence (such as $A_{14}G$) interfere with this stage of the folding process (Bassi *et al.*, 1995, 1996). The oligopurine stack might be regarded as the scaffold for the hammerhead structure; it is formed early in the folding process and it is the framework on which the complete structure is ultimately built. At the magnesium concentration of the intermediate structure, the ribozyme is essentially inactive (Dahm and Uhlenbeck, 1991), and we believe the catalytic core to be unfolded at this point. With the addition of further magnesium ions, in the 1–20 mM range, the orientation of helix I changes. Over the same range of magnesium concentrations the activity of the hammerhead ribozyme changes from being almost inactive to fully active (Dahm and Uhlenbeck, 1991), and it is probable that this stage reflects the folding of the catalytic core (domain I, or uridine turn) (Pley *et al.*, 1994; Scott *et al.*, 1995). Mutations in the $C_3U_4G_5A_6$ sequence (such as G_5C and deoxy G_5) (Bassi *et al.*, 1996) prevent the second stage of folding, but do not interfere with the first. This is summarized in Figure 8.

Ion binding and the first folding transition
Phosphorothioate interference experiments (Ruffner and Uhlenbeck, 1990) identified three phosphates [later shown to be *pro-R* oxygen atoms (Knoll *et al.*, 1997)] around the oligopurine stack region of domain II that were implicated in metal binding. These are the 5′ phosphates of A_9, A_{13} and A_{14}. These must all be regarded as candidates for the primary binding site for the metal ion that induces the first stage of folding. In the crystal structures (Pley *et al.*, 1994; Scott *et al.*, 1995), a metal ion has been consistently observed at the oligopurine stack of domain II, bound to the phosphate of A_9.

Ion binding and the second folding transition
Phosphorothioate substitution of the *pro-S* oxygen atom of A_6 has been shown to reduce the efficiency of self-cleavage by the hammerhead ribozyme (Knoll *et al.*, 1997). By rapid freezing of their hammerhead crystals,

Scott and coworkers (Scott *et al.*, 1996) have obtained a new structure in which further bound ions have been located. One of these is close to G_5, which is in good agreement with our earlier uranyl-induced photocleavage experiments (Bassi *et al.*, 1995). The location of this bound ion in the catalytic core makes it a candidate for the ion that induces the second stage of the folding process, i.e. the formation of the catalytic centre of the ribozyme. Mutation or modification of G_5 can prevent the second stage of folding (Bassi *et al.*, 1996). The guanine at this position is completely required for catalytic activity (Ruffner *et al.*, 1990), and alterations of specific functional groups lead to significant reduction in activity, including removal of the 2-amino group (Fu and McLaughlin, 1992b), the 6-carbonyl group (Tuschl *et al.*, 1993) and substitution by xanthine or isoguanine (Tuschl *et al.*, 1993). Removal of the 2′-hydroxyl group at G_5 markedly reduced catalytic activity (Fu and McLaughlin, 1992b), while repositioning the 2′OH by inversion of chirality at the $C_{2'}$ stereocentre led to an even larger reduction in activity (Fu *et al.*, 1994). The reduced catalytic activity of the deoxy G_5 hammerhead could be partially reversed by increasing the magnesium ion concentration (Fu and McLaughlin, 1992b). Grasby *et al.* (1993) found that the apparent affinity for magnesium of active hammerhead ribozyme was reduced 5-fold when G_5 was replaced by O^6-methylguanine.

Metal ion affinities
The association constant for the low-magnesium transition ($K = 8000$–$10\,000$ M^{-1}) is quite similar to that measured by Ohtsuka and coworkers (Koizumi and Ohtsuka, 1991), and is in the same range as the strongest association constant measured for magnesium binding to tRNA (Stein and Crothers, 1976). Eckstein and coworkers (Menger *et al.*, 1996) have studied magnesium-dependent trans-itions in the hammerhead by selective introduction of 2-aminopurine bases. Replacing $A_{1.1}$ with the fluorescent analogue, they measured a magnesium-dependent change in fluorescent quantum yield corresponding to an associ-ation constant $K = 505$ M^{-1}. This value is of the same order of magnitude as that measured in the second-stage transition. It is therefore likely that the 2-aminopurine, which is close to the point of self-cleavage, is sensitive to the folding of the catalytic core.

Structure and catalysis
It is likely that the two ion binding sites that we describe are essentially structural in function. Their role is probably twofold—to generate the correct local folded RNA geo-metry that facilitates the trajectory into the transition state, and to induce a structure that creates a new specific binding site for a catalytic metal ion(s). In the recent hammerhead structure obtained from frozen crystals, Scott and coworkers (Scott *et al.*, 1996) have identified a new bound magnesium ion attached to the *pro-R* oxygen at the cleaved phosphate at C_{17}. This ion is most probably distinct from the two that we have discussed, and is likely to participate in the chemistry of the cleavage reaction. The combination of structural strain and the positioning of one or more catalytic metal ions leads to the enhance-ment of the rate of cleavage of the phosphodiester bond.
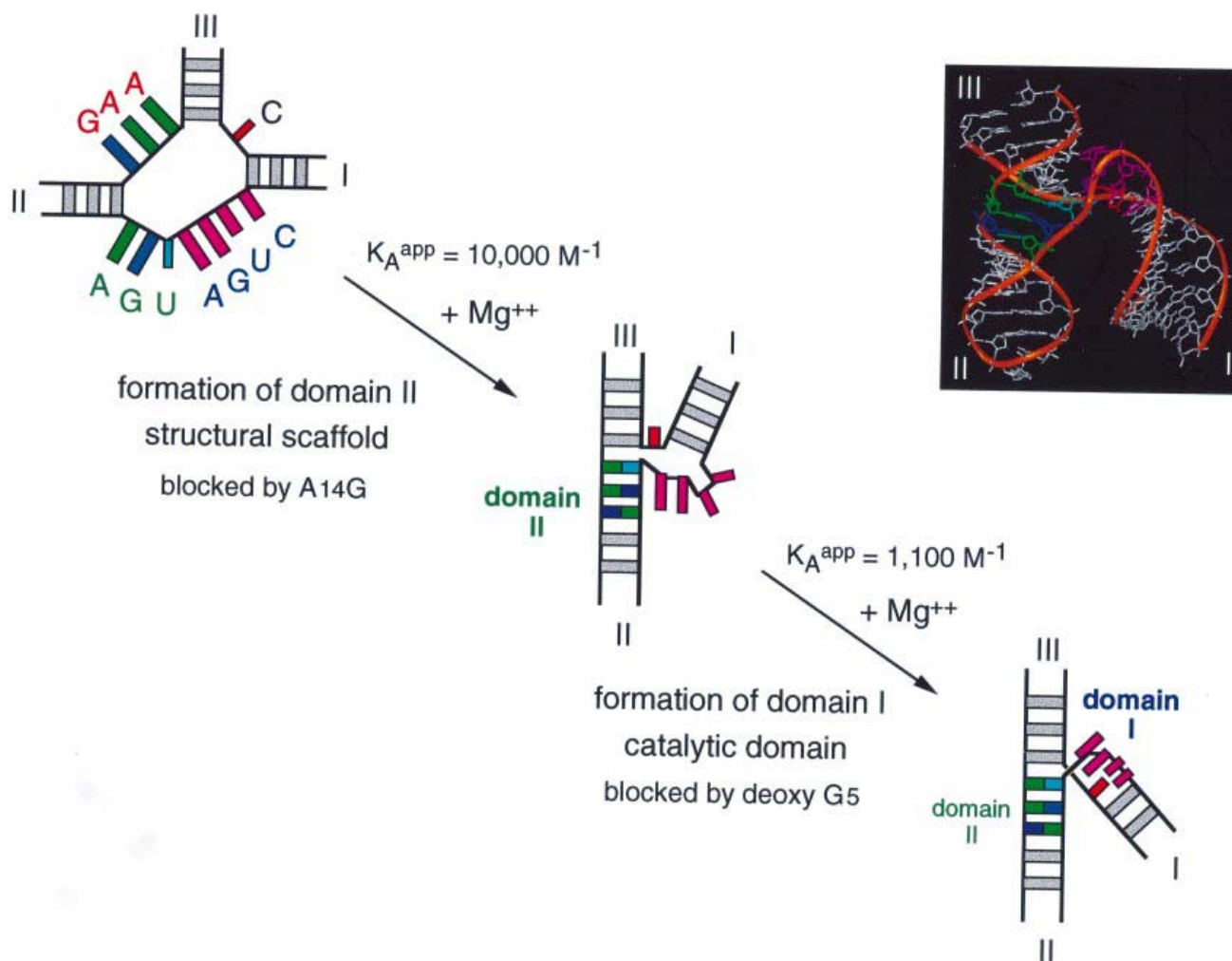
Fig. 8. Summary of the proposed two-stage ion-dependent folding process in the light of the crystal structures of the hammerhead ribozyme (Pley *et al.*, 1994; Scott *et al.*, 1995). The insert shows an image of the hammerhead molecule, generated from coordinates generously supplied by David McKay. This has been rotated into the same view as that used throughout this paper, and it can be seen that the global shape of the ultimate structures deduced from comparative gel electrophoresis and FRET are in good agreement with the crystal structures. The crystal structure comprises two domains. Domain II is formed by non-Watson–Crick pairings between G_{12}–A_9 and A_{13}–G_8, forming a coaxial stack between helices II and III that runs through the oligopurine sequence $G_{12}A_{13}A_{14}$. The adenine bases are coloured green, and the guanine bases blue. The catalytic domain is formed by the sequence $C_3U_4G_5A_6$ (coloured magenta), and the C_{17} of the substrate strand, where self-cleavage takes place, is coloured red. We suggest that the binding of the first structural ion (the low-magnesium ion transition occurring in the 0–600 µM range) induces the formation of domain II. The catalytic domain remains unfolded at this stage and hence helix I is oriented upwards in the view shown. Upon binding of a second structural magnesium ion (occurring in the concentration range 1–25 mM), the catalytic domain undergoes a folding transition, resulting in the rotation of helix I around into the same quadrant as helix II. Only at this stage does the hammerhead become a potentially active ribozyme.

Materials and methods

Synthesis of oligonucleotides
Oligonucleotides containing both DNA and RNA sections were synthesized using phosphoramidite chemistry (Beaucage and Caruthers, 1981) implemented on an Applied Biosystems 394 DNA/RNA synthesizer. RNA was synthesized using ribonucleotide phosphoramidites with 2′-*tert* butyldimethylsilyl (TBDMS) protection (Hakimelahi *et al.*, 1981; Perreault *et al.*, 1990) (Milligen). 6-Fluorescein (PE-ABI) and sulfoindocarbocyanine (Cy-3; Glen Research) were coupled to the 5′-termini as phosphoramidites. Oligoribonucleotides were deprotected in 25% ethanol/ammonia solution at 55°C for 6 h (dye labelled) or 12 h (unlabelled) and evaporated to dryness. Oligoribonucleotides were redissolved in 0.5 ml 1 M tetrabutylammonium fluoride (TBAF; Aldrich) in tetrahydrofuran to remove TBDMS groups, and agitated at 20°C in the dark for 16 h prior to desalting by G25 Sephadex (NAP columns; Pharmacia) and ethanol precipitation. Fully deprotected oligonucleotides were purified by gel electrophoresis in 20% polyacrylamide containing 7 M urea; fluorescently labelled species were significantly retarded in the gel system. Bands were excised, and the oligonucleotides were electroeluted into 8 M ammonium acetate and recovered by ethanol precipitation. Fluorescently labelled oligonucleotides were further puri-

fied by reverse phase HPLC. Samples were dissolved in 100 mM triethylammonium acetate (TEAAC) and applied to a C18 reverse phase column (µ Bondapak, Waters). The sample was eluted with a linear gradient of acetonitrile; buffer A: 100 mM TEAAC (pH 7.5), buffer B: acetonitrile, with a flow rate of 1 ml/min. Typical retention times were 20–30 min. The peak fractions were evaporated to dryness, redissolved in water and then ethanol precipitated.

Construction of hammerhead species for FRET analysis
The hammerhead constructs used in this study comprised the core and three arms each of 10 bp in length. The terminal base pair of each arm was DNA, as this allowed for a more efficient coupling of the fluorescent dye on the 5′ end of the molecule. The basic hammerhead species was constructed from three oligonucleotides:

Strand S (spanning stems III and I, 21 nt):

  5′ CGUAGUACGUCUGAGCGGUCG 3′

Strand R1 (spanning stems I and II, 27 nt):

  5′ CGACCGCUCACUGAUGAGGCCCACTCG 3′

Strand R2 (spanning arms II and III, 23 nt):

  5′ CGAGUGGGCCGAAACGUACUACG 3′

Underlined bases indicate deoxyribose substitution. For the FRET experiments, all versions of strand S contained deoxyribose substitution at C_{17} to prevent self-cleavage occurring in the presence of magnesium ions. In addition to these unlabelled oligonucleotides, each was synthesized with $5'$ fluorescein or Cy-3 fluorophores.

Hammerhead species for FRET studies were constructed from one unlabelled strand, one strand labelled with fluorescein and one Cy-3-labelled strand, thus placing the required fluorescein-Cy-3 pair at the ends of chosen arms. The molecules were hybridized by incubating stoichiometric amounts of the three appropriate RNA oligonucleotides in 90 mM Tris-borate (pH 8.3), 25 mM NaCl for 10 min at 80°C, followed by slow cooling. The hammerhead species were loaded onto a 12% polyacrylamide gel and electrophoresed at 4°C for 22 h at 150 V. The buffer system contained 90 mM Tris-borate (pH 8.3), 25 mM sodium chloride and was recirculated at >1 l/h. The fluorescent junctions were visualized by direct exposure to a standard lamp. The bands were excised and the RNA electroeluted into 8 M ammonium acetate and recovered by ethanol precipitation.

Analysis of self-cleavage

A substrate strand (S′) with full ribose-substitution in the core region was synthesized, and radioactively $5'$-^{32}P-labelled using $[\gamma$-^{32}P]ATP and polynucleotide kinase (Maxam and Gilbert, 1980).

Strand S′: $5'$ CGUAGUACGUCUGAGCGGUCG $3'$

S′ strand and ribozyme (an equimolar mixture of $5'$ fluorescein-labelled R1 and $5'$ Cy-3-labelled R2 strands) were prepared separately. Both solutions were heated in 50 mM Tris–HCl pH 8.0 at 70°C for 3 min and allowed to cool to 37°C. These were adjusted to a final concentration of 25 mM MgCl$_2$ and preincubated for 15 min at 37°C. The cleavage reaction was performed under single-turnover conditions, with a 100-fold excess of strands R1+R2 over strand S′. Cleavage was initiated by mixing the ribozyme and the substrate at 37°C. Aliquots were removed at different times and the reaction quenched with 80% formamide, 50 mM EDTA (pH 8.0) containing xylene cyanol and bromophenol blue at a temperature of 80°C. Cleavage was analysed by separation of substrate and products by electrophoresis in 20% polyacrylamide gels in 90 mM Tris-borate (pH 8.3), 2.5 mM EDTA containing 7 M urea. The extent of cleavage was estimated by exposure to storage phosphor screens and imaging (Fuji). The first order initial rate of cleavage was calculated by linear regression of ln (uncleaved/total S′) versus time.

An alkaline hydrolysis ladder was prepared by incubating the hammerhead RNA in 50 mM NaHCO$_3$, for 5 min at 90°C.

Fluorescence spectroscopy

Fluorescence emission spectra were measured on an SLM-Amino 8100 fluorimeter operating in photon counting mode, and spectra were corrected for lamp fluctuations and instrumental variations. Polarization artifacts were avoided by setting excitation and emission polarizers to magic angle conditions (54.74°). All spectra were recorded with samples thermostatted at 4°C in 5 mm cells.

FRET method

The rate constant for dipolar energy transfer is given by:

$$k_T = \frac{(R_0/R)^6}{\tau_D} \tag{5}$$

where τ_D is the lifetime of the donor in the absence of the acceptor, and R is the scalar separation of donor and acceptor.

$$R_0 = 8.785 \times 10^{-23} \, \Phi^D \cdot \kappa^2 \cdot \eta^{-4} \cdot J(\nu) \; \text{cm}^6 \tag{6}$$

where Φ^D is the fluorescent quantum yield of the donor in the absence of acceptor, $J(\nu)$ is the overlap integral between donor and acceptor, η is the refractive index of the medium and κ is the orientation factor for dipolar coupling. This can take values in the range 0–4; for rapid randomization of the relative donor-acceptor orientation, $\kappa^2 = 2/3$. The low anisotropy of RNA-conjugated fluorescein indicates that this is a reasonable approximation for the hammerhead constructs.

The efficiency of energy transfer (E_{FRET}) is given by:

$$E_{FRET} = \frac{1}{[1 + (R_0/R)^6]} \tag{7}$$

Analysis of fluorescence data

Efficiencies of energy transfer were determined from enhancement acceptor fluorescence (Clegg, 1992; Clegg *et al.*, 1992). The emission

at a given wavelength (ν_1) of a double-labelled sample excited primarily at the donor wavelength (ν') contains emission from the donor, emission from directly excited acceptor and emission from acceptor excited by energy transfer from the donor, i.e:

$$
\begin{aligned}
F(\nu_1,\nu') = [S] \cdot &\big[\varepsilon^D(\nu') \cdot \Phi_D(\nu_1) \cdot d^+ \cdot \{(1 - E_{FRET}) \cdot a^+ + a^-\} \\
&+ \varepsilon^A(\nu') \cdot \Phi_A(\nu_1) \cdot a^+ + \varepsilon^D(\nu') \cdot \Phi_A(\nu_1) \cdot E_{FRET} \cdot d^+ \cdot a^+\big] \\
= \; &F^D(\nu_1,\nu') + F^A(\nu_1,\nu') \tag{8}
\end{aligned}
$$

where [S] is the concentration of hammerhead molecules, d^+ and a^+ are the molar fraction of hammerhead molecules labelled with donor and acceptor respectively, and a^- is the molar fraction of hammerhead molecules unlabelled with acceptor. Superscripts D and A refer to donor and acceptor respectively. $\varepsilon^D(\nu')$ and $\varepsilon^A(\nu')$ are the molar absorption coefficients of donor and acceptor respectively and $\Phi^D(\nu_1)$ and $\Phi^A(\nu_1)$ are the fluorescent quantum yields of donor and acceptor respectively. Thus the spectrum contains the components due to donor emission $[F^D(\nu_1,\nu')$ i.e. the first term containing $\Phi^D(\nu_1)]$ and those due to acceptor emission $[F^A(\nu_1,\nu')$ i.e. the latter two terms containing $\Phi^A(\nu_1)]$.

The first stage of the analysis involves subtraction of the spectrum of RNA labelled only with donor, leaving just the acceptor components, i.e. $F^A(\nu_1, \nu')$. The pure acceptor spectrum thus derived is normalized to one from the same sample excited at a wavelength (ν'') at which only the acceptor is excited, with emission at ν_2. We then obtain the acceptor ratio:

$$
\begin{aligned}
(ratio)_A = \; &F^A(\nu_1,\nu')/F(\nu_2,\nu'') = \\
\big\{E_{FRET} \cdot d^+ \cdot &(\varepsilon^D(\nu')/\varepsilon^A(\nu'')) + (\varepsilon^A(\nu')/\varepsilon^A(\nu''))\big\} \cdot (\Phi_A(\nu_1)/\Phi_A(\nu_2)) \tag{9}
\end{aligned}
$$

E_{FRET} is directly proportional to $(ratio)_A$, and can be easily calculated since $\varepsilon^D(\nu')/\varepsilon^A(\nu'')$ and $\varepsilon^A(\nu')/\varepsilon^A(\nu'')$ are measured from absorption spectra, and $\Phi^A(\nu_1)/\Phi^A(\nu_2)$ is unity when $\nu_1 = \nu_2$.

Measurement of fluorescence anisotropy

Values of fluorescence anisotropy (r) were determined from measurements of fluorescence intensities using vertical excitation and emission polarizers ($F_\parallel$), and vertical excitation and horizontal emission polarizers ($F_\perp$). Fluorescence anisotropy was calculated from:

$$r = (F_\parallel - F_\perp)/(F_\parallel + 2F_\perp) \tag{10}$$

Absorption spectroscopy

Spectra of fluorophore-conjugated RNA were recorded between 220–650 nm on a Cary 1E spectrometer, from which absorption of RNA, fluorescein and Cy-3 could be determined.

Acknowledgements

References

Amiri,K.M.A. and Hagerman,P.J. (1994) Global conformation of a self-cleaving hammerhead RNA. *Biochemistry*, **33**, 13172–13177.

Bassi,G., Møllegaard,N.E., Murchie,A.I.H., von Kitzing,E. and Lilley,D.M.J. (1995) Ionic interactions and the global conformations of the hammerhead ribozyme. *Nature Struct. Biol.*, **2**, 45–55.

Bassi,G.S., Murchie,A.I.H. and Lilley,D.M.J. (1996) The ion-induced folding of the hammerhead ribozyme: core sequence changes that perturb folding into the active conformation. *RNA*, **2**, 756–768.

Beaucage,S.L. and Caruthers,M.H. (1981) Deoxynucleoside phosphoramidites—a new class of key intermediates for deoxypolynucleotide synthesis. *Tetrahedron Lett.*, **22**, 1859–1862.

Clegg,R.M. (1992) Fluorescence resonance energy transfer and nucleic acids. *Methods Enzymol.*, **211**, 353–388.

Clegg,R.M., Murchie,A.I.H., Zechel,A., Carlberg,C., Diekmann,S. and Lilley,D.M.J. (1992) Fluorescence resonance energy transfer analysis of the structure of the four-way DNA junction. *Biochemistry*, **31**, 4846–4856.

Clegg,R.M., Murchie,A.I.H., Zechel,A. and Lilley,D.M.J. (1993) Observing the helical geometry of double-stranded DNA in solution by fluorescence resonance energy transfer. *Proc. Natl Acad. Sci. USA*, **90**, 2994–2998.

Dahm,S.C. and Uhlenbeck,O.C. (1991) Role of divalent metal ions in the hammerhead RNA cleavage reaction. *Biochemistry*, **30**, 9464–9469.

Dahm,S.C., Derrick,W.B. and Uhlenbeck,O.C. (1993) Evidence for the role of solvated metal hydroxide in the hammerhead cleavage mechanism. *Biochemistry*, **32**, 13040–13045.

Duckett,D.R., Murchie,A.I.H., Diekmann,S., von Kitzing,E., Kemper,B. and Lilley,D.M.J. (1988) The structure of the Holliday junction and its resolution. *Cell*, **55**, 79–89.

Duckett,D.R., Murchie,A.I.H. and Lilley,D.M.J. (1995) The global folding of four-way helical junctions in RNA, including that in U1 snRNA. *Cell*, **83**, 1027–1036.

Eckstein,F. and Lilley,D.M.J. (1996) *RNA Catalysis.* Springer-Verlag, Berlin.

Epstein,L.M. and Gall,J.G. (1987) Self-cleaving transcripts of satellite DNA from the newt. *Cell*, **48**, 535–543.

Feldstein,P.A., Buzayan,J.M. and Bruening,G. (1989) Two sequences participating in the autolytic processing of satellite tobacco ringspot virus complementary RNA. *Gene*, **82**, 53–61.

Forster,A.C. and Symons,R.H. (1987) Self-cleavage of plus and minus RNAs of a virusoid and a structural model for the active sites. *Cell*, **49**, 211–220.

Fu,D.-J. and McLaughlin,L.W. (1992a) Importance of specific adenosine N^7-nitrogens for efficient cleavage by a hammerhead ribozyme. A model for magnesium binding. *Biochemistry*, **31**, 10941–10949.

Fu,D.-J. and McLaughlin,L.W. (1992b) Importance of specific purine amino and hydroxyl groups for efficient cleavage by a hammerhead ribozyme. *Proc. Natl Acad. Sci. USA*, **89**, 3985–3989.

Fu,D.J., Rajur,S.B. and McLaughlin,L.W. (1993) Importance of specific guanosine N^7-nitrogens and purine amino groups for efficient cleavage by a hammerhead ribozyme. *Biochemistry*, **32**, 10629–10637.

Fu,D.J., Rajur,S.B. and McLaughlin,L.W. (1994) Activity of the hammerhead ribozyme upon inversion of the stereocenters for the guanosine 2′-hydroxyls. *Biochemistry*, **33**, 13903–13909.

Gast,F.U., Amiri,K.M.A. and Hagerman,P.J. (1994) Interhelix geometry of stems I and II of a self-cleaving hammerhead RNA. *Biochemistry*, **33**, 1788–1796.

Grasby,J.A., Butler,P.J.G. and Gait,M.J. (1993) The synthesis of oligoribonucleotides containing O6-methylguanosine—the role of conserved guanosine residues in hammerhead ribozyme cleavage. *Nucleic Acids Res.*, **21**, 4444–4450.

Hakimelahi,G.H., Proba,Z.A. and Ogilvie,K.K. (1981) High yield selective 3′-silylation of ribonucleosides. *Tetrahedron Lett.*, **22**, 5243–5246.

Hampel,A. and Tritz,R. (1989) RNA catalytic properties of the minimum (–)sTRSV sequence. *Biochemistry*, **28**, 4929–4933.

Hazeloff,J.P. and Gerlach,W.L. (1988) Simple RNA enzymes with new and highly specific endoribonuclease activities. *Nature*, **334**, 585–591.

Hertel,K.J. *et al.* (1992) Numbering system for the hammerhead. *Nucleic Acids Res.*, **20**, 3252.

Hutchins,C.J., Rathjen,P.D., Forster,A.C. and Symons,R.H. (1986) Self-cleavage of plus and minus RNA transcripts of avocado sunblotch viroid. *Nucleic Acids Res.*, **14**, 3627–3640.

Klement,R., Soumpasis,D.M. and Jovin,T.M. (1991) Ionic distributions around charged biomolecular structures. Results for right-handed and left-handed DNA. *Proc. Natl Acad. Sci. USA*, **88**, 4631–4635.

Knoll,R., Bald,R. and Fürste,J.P. (1997) Complete identification of nonbridging phosphate oxygens involved in hammerhead cleavage. *RNA*, **3**, 132–140.

Koizumi,M. and Ohtsuka,E. (1991) Effects of phosphorothioate and 2-amino groups in hammerhead ribozymes on cleavage rates and Mg^{2+} binding. *Biochemistry*, **30**, 5145–5150.

Lilley,D.M.J., Clegg,R.M., Diekmann,S., Seeman,N.C., von Kitzing,E. and Hagerman,P. (1995) Nomenclature committee of the International Union of Biochemistry: A nomenclature of junctions and branchpoints in nucleic acids. Recommendations 1994. *Eur. J. Biochem.*, **230**, 1–2.

Maxam,A.M. and Gilbert,W. (1980) Sequencing end-labelled DNA with base-specific chemical cleavages. *Methods Enzymol.*, **65**, 499–560.

Menger,M., Tuschl,T., Eckstein,F. and Porschke,D. (1996) Mg^{2+}-dependent conformational changes in the hammerhead ribozyme. *Biochemistry*, **35**, 14710–14716.

Murchie,A.I.H., Clegg,R.M., von Kitzing,E., Duckett,D.R., Diekmann,S. and Lilley,D.M.J. (1989) Fluorescence energy transfer shows that the four-way DNA junction is a right-handed cross of antiparallel molecules. *Nature*, **341**, 763–766.

Olsen,D.B., Benseler,F., Aurup,H., Pieken,W.A. and Eckstein,F. (1991) Study of a hammerhead ribozyme containing 2′-modified adenosine residues. *Biochemistry*, **30**, 9735–9741.

Paolella,G., Sproat,B.S. and Lamond,A.I. (1992) Nuclease resistant ribozymes with high catalytic activity. *EMBO J.*, **11**, 1913–1919.

Perreault,J.-P., Wu,T., Cousineau,B., Ogilvie,K.K. and Cedergren,R. (1990) Mixed deoxyribo- and ribooligonucleotides with catalytic activity. *Nature*, **344**, 565–567.

Pley,H.W., Flaherty,K.M. and McKay,D.B. (1994) Three-dimensional structure of a hammerhead ribozyme. *Nature*, **372**, 68–74.

Ruffner,D.E. and Uhlenbeck,O.C. (1990) Thiophosphate interference experiments locate phosphates important for the hammerhead RNA self-cleavage reaction. *Nucleic Acids Res.*, **18**, 6025–6029.

Ruffner,D.E., Stormo,G.D. and Uhlenbeck,O.C. (1990) Sequence requirements of the hammerhead RNA self-cleavage reaction. *Biochemistry*, **29**, 10695–10702.

Scott,W.G., Finch,J.T. and Klug,A. (1995) The crystal structure of an all-RNA hammerhead ribozyme: A proposed mechanism for RNA catalytic cleavage. *Cell*, **81**, 991–1002.

Scott,W.G., Murray,J.B., Arnold,J.R.P., Stoddard,B.L. and Klug,A. (1996) Capturing the structure of a catalytic RNA intermediate: The hammerhead ribozyme. *Science*, **274**, 2065–2069.

Seela,F., Mersmann,K., Grasby,J.A. and Gait,M.J. (1993) 7-Deazaadenosine—oligoribonucleotide building block synthesis and autocatalytic hydrolysis of base-modified hammerhead ribozymes. *Helv. Chim. Acta*, **76**, 1809–1820.

Sharmeen,L., Kuo,M.Y., Dinter-Gottlieb,G. and Taylor,J. (1988) Antigenomic RNA of human hepatitis delta virus can undergo self-cleavage. *J. Virol.*, **62**, 2674–2679.

Sigurdsson,S.T., Tuschl,T. and Eckstein,F. (1995) Probing RNA tertiary structure: interhelical crosslinking of the hammerhead ribozyme. *RNA*, **1**, 575–583.

Slim,G. and Gait,M.J. (1991) Configurationally defined phosphoro-thioate-containing oligoribonucleotides in the study of the mechanism of cleavage of hammerhead ribozymes. *Nucleic Acids Res.*, **19**, 1183–1188.

Stein,A. and Crothers,D.M. (1976) Equilibrium binding of magnesium (II) by *Escherichia coli* tRNAfMet. *Biochemistry*, **15**, 157–160.

Thomson,J.B., Tuschl,T. and Eckstein,F. (1996) The hammerhead ribozyme. In Eckstein,F. and Lilley,D.M.J. (eds), *Nucleic Acids and Molecular Biology.* Springer Verlag, Vol. 10, pp. 173–196.

Tuschl,T., Ng,M.M.P., Pieken,W., Benseler,F. and Eckstein,F. (1993) Importance of exocyclic base functional groups of central core guanosines for hammerhead ribozyme activity. *Biochemistry*, **32**, 11658–11668.

Tuschl,T., Gohlke,C., Jovin,T.M., Westhof,E. and Eckstein,F. (1994) A three-dimensional model for the hammerhead ribozyme based on fluorescence measurements. *Science*, **266**, 785–789.

Uhlenbeck,U.C. (1987) A small catalytic oligoribonucleotide. *Nature*, **328**, 596–600.

van Tol,H., Buzayan,J.M., Feldstein,P.A., Eckstein,F. and Bruening,G. (1990) Two autolytic processing reactions of a satellite RNA proceed with inversion of configuration. *Nucleic Acids Res.*, **18**, 1971–1975.

Welch,J.B., Walter,F. and Lilley,D.M.J. (1995) Two inequivalent folding isomers of the three-way DNA junction with unpaired bases: sequence-dependence of the folded conformation. *J. Mol. Biol.*, **251**, 507–519.

Williams,D.M., Pieken,W.A. and Eckstein,F. (1992) Function of specific 2′-hydroxyl groups of guanosines in a hammerhead ribozyme probed by 2′-modifications. *Proc. Natl Acad. Sci. USA*, **89**, 918–921.

Yang,J.-H., Usman,N., Chartrand,P. and Cedergren,R. (1992) Minimum ribonucleotide requirement for catalysis by the RNA hammerhead domain. *Biochemistry*, **31**, 5005–5009.